Mg 2+ −Free Bacillus stearothermophilus Tryptophanyl-tRNA Synthetase Retains a Major Fraction of the Overall Rate Enhancement for Tryptophan Activation

ARTICLE *in* JOURNAL OF THE AMERICAN CHEMICAL SOCIETY · JANUARY 2008

Impact Factor: 12.11 · DOI: 10.1021/ja076557x · Source: PubMed

2 AUTHORS:

Violetta Weinreb
University of North Carolina at Chapel Hill
16 PUBLICATIONS **255** CITATIONS
SEE PROFILE

Charles W Carter
University of North Carolina at Chapel Hill
110 PUBLICATIONS **11,417** CITATIONS
SEE PROFILE

Published in final edited form as:
J Am Chem Soc. 2008 January 30; 130(4): 1488–1494. doi:10.1021/ja076557x.

Mg^{2+}-free *B. stearothermophilus* Tryptophanyl-tRNA Synthetase Retains a Major Fraction of the Overall Rate Enhancement for Tryptophan Activation

Violetta Weinreb and **Charles W. Carter Jr***
Department of Biochemistry and Biophysics CB 7260 University of North Carolina, Chapel Hill, NC. 27599-7260

Abstract

Few experimental data are available for rates of enzymatic phosphoryl-transfer reactions in the absence of the divalent metal ions associated with such reactions. Such data are of interest for amino acid activation by class Ic aminoacyl-tRNA synthetases, for which there is substantial evidence that binding energy of ATP may account for a major fraction of the overall rate enhancement, and it is crucial to know if these effects themselves depend on the divalent metal ion. We describe a nested, non-linear model for the sum of metal-free and metal-catalyzed activities and its use in determining metal-free enzyme activity jointly with transition-state metal binding affinity, by fitting observed values obtained from Mg^{2+}-depleted assays with increasing [EDTA] at known $[Mg^{2+}]_{total}$. Tryptophan activation by *B. stearothermophilus* tryptophanyl-tRNA synthetase falls asymptotically to a plateau value five orders of magnitude below that observed for the Mg^{2+}-supplemented enzyme at EDTA concentrations that reduce the free metal concentration to <1 pmolar. The fitted regression model parameters yield a relative rate acceleration of 9.3×10^4 attributable to the catalytic effect of Mg^{2+} and an enhanced ($K_E^{\ddagger} = 1.15 \times 10^{-7}$ M) transition-state binding of Mg^{2+}. Factorial analysis indicates that 80% of the reduction in free energy of activation effected by TrpRS arises from protein-ligand interactions.

INTRODUCTION

Enzymatic phosphoryl transfer reactions almost invariably involve one or more divalent Mg^{2+} ions, consistent with the inevitable increase in negative charge that develops in their transition states. However, Mg^{2+} itself has little effect on non-enzymatic rates[1], and reports of the rate acceleration attributable to the divalent metal differ markedly for different enzymes. Empirical valence bond simulations of two nuclease mechanisms[2] suggest that the metal contributes > 10 orders of magnitude in rate enhancement to phosphodiester bond hydrolysis catalyzed by enzymes using one[3] and two[4] Mg^{2+} ions. In contrast, protein farnesyl transferase loses only three orders of magnitude in rate enhancement when Mg^{2+} is excluded[5].

The question of how Mg^{2+} contributes to rate enhancement is especially interesting for the amino acid activation reaction catalyzed by class Ic aminoacyl-tRNA synthetases (aaRS) for tyrosine and tryptophan. Uncatalyzed amino acid activation has not been measured. However, reaction of acetate with p-NO phenyl phosphate provides a good model for amino acid activation[6]. That reaction proceeds at 8.3×10^{-9}/mol/sec[7,8], and comparison with k_{cat}/Km for amino acid activation, ~10^6 /mol/sec[9] leads to a rate acceleration of ~10^{14}. A fuller understanding of catalytic contributions may come from quantum mechanical simulations[10],

*CORRESPONDING AUTHOR FOOTNOTE Tel: 919 966-3263; FAX: 919 966-2852; carter@med.unc.edu.

which will benefit from calibration by experimentally determined constraints, including parameters associated with the role of divalent metals.

Fersht's work on the class I tyrosyl-tRNA synthetase (TyrRS)[11] showed that much of its catalytic rate enhancement derives from the binding free energy of ATP. Our work on the closely related tryptophanyl-tRNA synthetase (TrpRS) provided crucial structural data clarifying that suggestion. We pointed out that the residues homologous to those shown to develop high transition-state affinity in TyrRS were located in subsites for the adenosine and pyrophosphate (PPi) moieties of ATP, and that these subsites are very likely moving substantially, relative to one another in a dynamic transition state between the pre-transition state (PreTS) ATP complexes (1MAU and 1M83) and the Trp-5'AMP Products complexes (1I6K, 1I6L, and 1I6M). Thus, both mechanistic enzymology and structural studies of TyrRS and TrpRS have implicated major catalytic roles for ground-state conformational destabilization and nucleotide and pyrophosphate moiety binding free energies distributed far from the scissile bond and in class Ic aaRS catalysis9،11–15.

The two notions of distributed catalytic use of ATP binding energy[11,15] and relative movement of different subsites[16] at precisely the moment they develop highest affinity, comprise novel evidence for a source of catalytic power – strain - that had been widely discounted because of the “soft” characteristics of the forces a protein can apply directly to a scissile bond[17]. The case for strain is strengthened[15] by the experimental determination of the positive conformational free energy change associated with assembling the PreTS state during induced-fit and by the improved binding to adenosine and pyrophosphate moieties of the transition state analog inhibitor, adenosine-5'tetraphosphate, AQP.

Moreover, the best crystallographic evidence[14] indicates that the metal in PreTS TrpRS•Mg^{2+}•ATP complexes (1MAU, 1M83) binds only to three non-bridging phosphate oxygen atoms and two water molecules. None of the potential protein ligands is within ~3.5 Å of the metal. This configuration resembles that of Mg^{2+}•ATP in water[18]. Without actually interacting directly with the metal, TrpRS provides an environment capable of activating the configuration of aqueous Mg^{2+}•ATP to one in which Mg^{2+} can substantially accelerate the rate of phosphoryl transfer.

These studies emphasize the importance of determining the catalytic contribution of Mg^{2+} experimentally. As the metal makes no direct contact with the protein in any of the observed ground-state structures, and hence cannot effect protein stability, catalytic activity observed in its absence would allow an unambiguous distinction to be made between the catalytic contributions of protein-ligand interaction energies, those of the metal, and those arising from interactions between them by factorial analysis. It is thus of considerable interest to determine as quantitatively as possible the catalytic importance of the single divalent metal[14] implicated in amino acid activation by these enzymes.

Experimental study of this question is beset by several difficulties. First, Mg^{2+} appears to bind tightly only to the activated PreTS complex with amino acid and ATP[14]. Steady-state kinetic measurements afforded an estimate of 2 μM for the Km for Mg^{2+}, or the ground-state dissociation constant of the metal from the enzyme:ATP complex for *B. stearothermophilus* tryptophanyl-tRNA synthetase (TrpRS)[14] in the PreTS state. This affinity is similar to the dissociation constant of Mg^{2+} from ATP (7 □M;19), suggesting that the enzyme itself has little net effect on that equilibrium. The affinity is, however, high enough to complicate experiments to determine residual catalytic activity in the absence of the metal, because methods of determining free metal ion concentrations are insensitive below 100 μM20, so we are limited to measuring analytically the total [Mg^{2+}].

A second difficulty arises because the Mg^{2+} affinity of the active site may increase during the transition state. Scavenging from a small amount of free metal ion by a tight-binding transition state may lead to activity at quite low Mg^{2+} concentrations (Figure 1). For any known, limiting $[Mg^{2+}]_{total}$, two unknown constants therefore determine the observed rates: the ratio of the metal-catalyzed to the metal-free enzymatic rate, and the affinity of the transition state for Mg^{2+}. Both parameters must therefore be determined jointly.

RESULTS

We address these difficulties by analyzing the observed TrpRS PPi-exchange activity in Mg^{2+}-depleted solutions whose total $[Mg^{2+}]$ is known, as a function of increasing [EDTA]. Treatment of assay buffers and enzyme with Chelex 100, a standard procedure to eliminate metals[21] reduces TrpRS activity roughly 100-fold14. Successive additions of EDTA reduce this activity by another factor of at least 100 (Figure 1A). The activity approaches asymptotically a value well within the sensitivity of the assay, suggesting that a major portion of TrpRS catalytic activity at high [EDTA] derives from metal-free enzyme. We verified this conclusion by quantitative modeling of the observed activity as a linear combination of metal-free and metal-catalyzed TrpRS activity.

We fit a nested, bivariate, nonlinear model for the TrpRS•ATP•Mg^{2+} concentration and the total activity to the observed values (Figure 1) by iterative least squares estimation to obtain estimates for the two parameters (Table 1) from the [EDTA]-dependence of the observed activity. As described in greater detail under *Calculations*, the observed activity depends on the proportion and relative activity of Mg^{2+}-free TrpRS in each assay. The latter is an explicit parameter in expressing the total activity as the sum of Mg^{2+} assisted and Mg^{2+}-free activities. The former, however depends explicitly on solutions to the two simultaneous quadratic equations arising from equilibria describing interaction of Mg^{2+} with EDTA and enzyme, respectively, and implicitly on the affinity of Mg^{2+} for the TrpRS•ATP transition state complex (see Figures 3 and 4). From the fitting, we find Mg^{2+}-independent TrpRS catalysis at rates 9×10^8 times faster than the estimated rate of the uncatalyzed reaction.

Moreover, consistent with the likely transient increase in negative charge, we also find that the affinity of the TrpRS active site for Mg^{2+} increases, (~20-fold; 60-fold over the affinity of ATP for Mg^{2+}) in the transition state. As noted below, these parameters are conservative estimates for the magnitudes of the overall rate enhancement achieved by metal-free TrpRS and the affinity of the reacting protein:ATP complex for Mg^{2+}, both of which are likely somewhat higher, because weaker Mg^{2+}-binding equilibria omitted from explicit modeling would decrease estimates of $[Mg^{2+}]_{free}$.

The data in Figure 1 and Table 1, together with the activity of the enzyme with Mg^{2+} and estimates for the uncatalyzed reaction[6] and the effect of Mg^{2+} alone[1], complete a thermodynamic cycle or two-way factorial experiment describing the catalytic effects of enzyme and Mg^{2+}. We used the multiple measurements of Mg^{2+}-free and Mg^{2+}-activated activity, together with published values for the rates in water, ± Mg^{2+} in a factorial regression model to estimate the two mean effects and their interaction (Figure 2). The mean effect of the enzyme with and without Mg^{2+} is −15.6 kcal/mole, or ~80% of the total reduction in free energy at the transition state. The Mg^{2+} itself stabilizes the transition state by an average of −3.7 kcal/mol, but this effect is very disproportionate, as the two-way interaction term, $\Delta(\Delta G^{\ddagger})_{int}$, −6.4 kcal/mol, is of the same magnitude as the effect of Mg^{2+} on the enzyme-catalyzed reaction. Thus, essentially all of the contribution of the divalent metal to catalytic rate enhancement arises from the environment created for it by the enzyme and is accomplished without direct, ground-state protein-metal bonds. We cannot rule out the possibility that in the transition state

active-site rearrangement leads to transient bonds between the metal and, for example, the nearby aspartate residues D146[11] or D197[12].

DISCUSSION

The high, and *a priori* unknown affinity of an enzyme•ATP complex for Mg^{2+} means that metal-independent catalytic activity cannot be determined without simultaneously determining that affinity. We show here how both parameters can be estimated jointly by modeling the activity measured at different EDTA concentrations assuming known affinity of the metal•EDTA complex. The small concentrations of free Mg^{2+} in the assays mean that they cannot be measured experimentally and therefore must be determined by quantitative modeling from known total Mg^{2+} concentrations, which we determined analytically (Table 2). Not surprisingly, the two parameters are highly correlated: their interaction ($R \times K_E^{\ddagger}$) dominates the elliptical shape of the SSE response surface, which has an axial ratio of roughly two (Table I, column 4), contributing to significant percent error in the fitted parameters. Thus, use of two different protein concentrations provided an important additional constraint for reliable parameter estimation.

As Mg^{2+} ion is not coordinated by active-site functional groups in any of the known crystal structures, the transient increase in transition state Mg^{2+} affinity occurs in a structural context that leaves the metal relatively free to migrate significantly during the course of the reaction. The actual transition state configuration in TrpRS tryptophan activation and hence the structural location of the metal in the transition state are unknown and probably differ from what is seen in the TrpRS crystal structures.

Phosphoryl transfer reactions generally fall into two categories, called associative or dissociative according to the degree of bond-making and bond-breaking in the transition state. This distinction, in turn, determines the distribution of negative charge throughout the transition state[22]. The increased transition state affinity and likely Mg^{2+} movement are both consistent with several structural data that argue for dissociative character in the transition state[15]. Associative transition states develop significant additional negative charge primarily on the non-bridging α-phosphate oxygen atoms, while the TrpRS active site provides little direct interaction with the α-phosphate that might accommodate such additional charge. Dissociative character, on the other hand, entails increased negative charge largely on the PPi leaving group, precisely where the Mg^{2+} and TrpRS active-site lysine residues are positioned to contribute most effectively.

Further, dissociative character would involve greater relative movement of the PPi leaving group, and formation of the TrpRS Products complex[23,24] entails substantial relative movement of the ribose and PPi binding subsites away from each other, relative to the configuration in the PreTS state.

Finally, AQP, though not a substrate, binds two orders of magnitude more tightly to a TrpRS conformation intermediate between the PreTS and Products states[15]. In that complex, the γ- and δ-phosphates mimic the leaving PPi group. Doing so, they mimic dissociative character by the increased physical separation from the adenosine monophosphate moiety. The PPi mimic and adenosine both form improved binding interactions with the new locations of their respective binding sites. In particular, the terminal PPi mimic interacts strongly with the KMSKS loop, suggesting that movement of the loop enables it to better accommodate a transition state with dissociative character, in keeping with the two previous observations.

The distribution of interactions responsible for the higher affinity of AQP throughout the adenosine and PPi-binding subsites is fully consistent with extensive mutational data for the homologous TyrRS system[11], which implicated comparable interactions in transition state

binding. The available evidence thus suggests that the transition state entails significant dissociative character, and implies that the α-phosphate assumes a metaphosphate-like transition-state configuration. The enhanced affinity for Mg^{2+} is therefore likely to involve increased negative charge on the leaving group, in keeping with its predominant interactions with the β- and γ-phosphate oxygen atoms in the ground-state complexes 1MAU and 1M83.

The parameter, $R = 1.07 \times 10^{-5}$ implies that TrpRS accelerates tryptophan activation by ~ 10^9–fold in the absence of Mg^{2+}. Values for the Mg^{2+} affinity and relative rate enhancement parameters will provide important experimental calibration for quantum mechanical simulations of the catalyzed reaction[10]. Such computational approaches may eventually provide a more complete picture of the catalytic transition.

The substantial Mg^{2+}-independent rate acceleration must be achieved by transition-state stabilization mechanisms other than electrostatic charge compensation by the divalent metal. What mechanisms might act catalytically in its absence? At least three distinct sources could contribute to Mg^{2+}-independent catalysis[15]. First, hydrogen bonding in the transition state by the backbone amide group of residue Q9 may stabilize negative charge developed on the non-bridging oxygen atom OA1 in a metaphosphate configuration of the α-phosphate group. A similar effect was observed in the genetic dissection of the subtilisin hydrolytic mechanism[25], where a residual rate acceleration of 10^3 when the catalytic triad was ablated was attributed to the “oxyanion hole” created by main chain hydrogen bonding and hence not easily mutated. Such stabilization would be Mg^{2+}-independent.

Additional catalytic effects arise from the TIGN and KMSKS loops[26,27]. For the closely related TyrRS, mutation of these two signatures reduces k_{cat} with minimal effects on Km, consistent with transient strengthening of binding interactions to the ribose and PPi moieties in the transition state. As noted above, AQP binds to TrpRS in the absence of Mg^{2+} with substantially higher affinity than does ATP. AQP interacts with both signatures in a manner suggesting the distributed origins of enhanced transition state affinity in the native enzyme[15]. The 200-fold greater affinity of AQP, relative to Mg^{2+}•ATP, suggests that these distributed interactions could accelerate the reaction by at least two orders of magnitude in the absence of Mg^{2+}.

The free energy cost of induced-fit is +3.0 Kcal/mole[15] and represents potential catalytically relevant ground-state destabilization by a factor of ~150. The exergonic untwisting domain motion observed when the TrpRS pre-transition state converts to the Products conformation and which relocates the PPi leaving group recovers much, if not most of this conformational strain[28]. The recovered free energy and the strengthening of interactions to PPi in the AQP complex imply that breaking the bond between the bridging oxygen atom and the α-phosphorus allows the leaving group to form stronger bonds to the KMSKS loop as it rotates away from the α-phosphate, likely accompanied by the Mg^{2+} ion, which is not present in the Product complex with Trp-5'AMP[23,24].

The induced-fit and catalytic domain motions therefore represent storage and recovery of conformational free energy that likely is used for catalysis by the native enzyme. Complementary experimental evidence for the catalytic contribution of these conformational effects comes from the ~ 10^5-fold reduction in rate enhancement, in the presence of Mg^{2+}, when two-thirds of the native enzyme mass is deleted, leaving a nearly intact, minimal catalytic domain[29].

Together, these three distinct potential sources of rate acceleration (3×10^7) could account for much of the 10^9-fold rate enhancement in the absence of Mg^{2+}. The first two sources are likely Mg^{2+}-independent. However, the ground-state destabilization arising during induced-fit is probably Mg^{2+}-dependent[28]. Thus, if it does contribute, then it does so by a different mechanism.

CONCLUSIONS

We demonstrate that a considerable (i.e., at least 9 orders of magnitude) rate enhancement for tryptophan activation is intrinsic to the TrpRS catalytic site. Analytical $[Mg^{2+}]_{Total}$ determinations and multiple TrpRS concentrations provide important constraints for the multidimensional fitting of calculated to observed activities and parameter estimation. In particular, the regression model affords for the first time an experimental lower limit, $K_E^{\ddagger} = 1.1 \times 10^{-7}$, for the strength with which the catalytic Mg^{2+} is bound in the transition state. The high Mg^{2+}-independent catalytic activity is unexpected in light of the almost invariant association of this metal with phosphoryl-transfer reactions. The large $\Delta(\Delta G^{\ddagger}_{int})$ term from the thermodynamic cycle in Figure 2 implies that in addition to metal-independent catalysis, TrpRS-Ligand interactions are also required in order for rate enhancement by Mg^{2+}, leading to the conclusion that 80% of the catalytic rate enhancement arises from the protein itself.

EXPERIMENTAL SECTION

The assay buffer (0.1M Tris-Cl, 0.01M KF, 2mM ATP, 2mM Tryptophan, 70 mM 2-mercaptoethanol pH 8.0) was treated with Chelex 100 for 30 min at 4°C with shaking to remove Mg^{2+} ion[21]. Then equal 190 μl volumes were aliquoted for assaying triplicates of all samples and blanks. To each aliquot we added different amounts of EDTA (none, 0.01 mM, 0.05 mM, 0.1 mM, 0.5 mM, 1.0 mM, 2.0 mM, 5.0 mM). To each assay was added ^{32}PPi to 2 mM at a specific radioactivity between 1×10^5 and 2×10^5 CPM/□M. All assays were done at 37°C. The reaction was initiated by adding 10 μl TrpRS to total concentrations of either 4.5 μM or 13.2 μM to the mix, which was incubated for 15 (+Mg^{2+}) or 90 (−Mg^{2+}) minutes at 37°C, quenched with 7% Perchloric Acid on ice with the addition of 50 □| of 15% Norit A, and filtered through Amicon Ultrafree-MC centrifugal filter devices (Cat UFC30GVNB). Then they were washed with 15 ml of deionized water. All samples were incubated with 50 □| of Pyridine for 15 min at 37°C, then pyridine was collected by centrifugation and counted for ten minutes with 5ml of scintillation solution Ecoscint A. All assay components were also analysed by Inductively Coupled Plasma Optical Emission Spectroscopy (ICP-OES) (Table 2) to determine residual Mg^{2+} concentrations.

CALCULATIONS

The model for least squares parameter estimation

In a regime of decreasing $[Mg^{2+}_{free}]$, both Mg^{2+}-bound TrpRS•Mg^{2+}•ATP, whose specific activity, Act_{+Mg}, is known experimentally but whose concentration is unknown, and Mg^{2+}-free enzyme, [TrpRS•ATP], whose specific activity and concentration are both unknown, may contribute in different proportions to total observed activity. For a known total enzyme concentration, only one of the two enzyme concentrations need be determined. For example, if the [TrpRS•Mg^{2+}•ATP] has been determined, the total observed activity, Act_{obs}, can be expressed in terms of the Mg^{2+}-bound and total enzyme concentrations and an adjustable parameter, the ratio, R, of the Mg^{2+}-free activity to that of the Mg^{2+}-bound activity (I):

$$Act_{obs} = Act_{+Mg}{}^{*}\left(\left[\mathrm{TrpRS} \bullet Mg^{2+} \bullet \mathrm{ATP}\right] + R^{*}\left\{\left[\mathrm{TrpRS}_{tot}\right] - \left[\mathrm{TrpRS} \bullet Mg^{2+} \bullet \mathrm{ATP}\right]\right\}\right) \quad \text{(I)}$$

For any $[Mg^{2+}_{tot}]$, four coupled equilibria determine $[Mg^{2+}_{free}]$ in assays of pyrophosphate exchange in the presence of known amounts of EDTA. EDTA itself, TrpRS•ATP, ATP, and PPi all have significant affinities for free Mg^{2+} ion. Each equilibrium can be expressed in terms of the total compound concentration, an appropriate dissociation constant, the $[Mg^{2+}_{free}]$, and the sum of all Mg^{2+}-bound forms, which is the same for all of the coupled equilibria. Under a regime of decreasing [Mg^{2+}Total], each of the four equilibria will contribute in different

proportions to the [Mg^{2+}_{free}] and hence to the overall activity. Stability constants from the literature differ somewhat. For consistency, we list in Table 3 the dissociation constants for these compounds as listed by Sillen and Martell[30], which are quite similar to those cited by Patton[31].

At first glance the situation appears straightforward: Mg^{2+} binding by EDTA should compete orders of magnitude more strongly with each of the three remaining equilibria, because the ATP, PPi, and TrpRS•ATP complex all bind Mg^{2+} with approximately the same affinity, three orders of magnitude more weakly than EDTA. Under such circumstances, only the [EDTA] need be explicitly incorporated into calculations of the free [Mg^{2+}] with increasing [EDTA].

Results in Figure 1 suggest, however, that this view is inappropriate: Chelex 100 treatment leaves a [Mg^{2+}total] concentration of ~600 nM in the assays, with some variation from the Mg^{2+} introduced with differing amounts of EDTA. This amount is below the dissociation constants for any of the assay components and well above that for EDTA. Thus, in the absence of additional EDTA, there is likely sufficient free Mg^{2+} to generate appreciable activity from the TrpRS•Mg•ATP complex.

Consistent with that expectation, the observed activity declines over a > 400-fold range of additional EDTA concentrations, which have no effect on the reaction supplemented by 10 mM Mg^{2+} (Figure 1A). We conclude that activity from the Mg^{2+}-activated enzyme ATP complex persists under these conditions, contributing successively less to the observed activity, despite the fact that equilibrium calculations indicated that the EDTA concentrations should reduce the free [Mg^{2+}] to below 10^{-12} M. The remaining activity, together with the ~10^4–fold ratio between the Mg^{2+}-supplemented and Mg^{2+}-depleted reactions at the highest [EDTA] implicate competition for metal between TrpRS•ATP and chelator at [Mg^{2+}_{free}] values smaller than those required to activate the equilibria listed in Table 3. Thus, the data plotted in Figure 1 are conditioned by two unknown quantities: the dissociation constant of Mg^{2+} from the TrpRS•Mg^{2+}•ATP transition-state complex, and the ratio of metal activated and metal-independent activity, as shown in Figure 3.

We assume to a first approximation that pyrophosphate, ATP, and ground-state TrpRS•ATP Mg^{2+} affinities in Table 2 may be neglected, because the most important competition occurs between EDTA and activated [TrpRS•ATP] whose (unknown) affinity exceeds the ground-state affinity measured by steady state kinetics. This assumption avoids modeling three weaker equilibria in assessing the free [Mg^{2+}]. Modeling all equilibria simultaneously by including bound forms of ATP and PPi, would involve solving additional simultaneous quadratic equations. Correcting the error caused by this simplification, would reduce the [Mg^{2+}_{free}] and hence strengthen the estimated affinity of the transition-state TrpRS•ATP•Mg^{2+} complex, and increase the estimated R. The simplification will therefore lead to an upper limit to the dissociation constant for the TrpRS complex and a lower limit for R.

Assuming that the enzyme is saturated with ATP, the two remaining quadratic expressions involving [Mg^{2+}_{free}] can be solved iteratively from the known total enzyme, chelator, and metal concentrations, enabling calculation of [TrpRS•ATP•Mg^{2+}] and Mg^{2+}-free [TrpRS•ATP]. These values are necessary and sufficient to evaluate the [EDTA] dependence of the observed catalytic activity (Figure 3) by adjusting the TrpRS•ATP‡ transition-state Mg^{2+} affinity, $K_E^{‡}$, and the activity ratio, R. Let x = [EDTA•Mg], y = [TrpRS*Mg•ATP], D_{tot} = $[EDTA]_{total}$, $[Mg^{2+}]_{tot}$ = $[Mg^{2+}]_{total}$, and E_{tot} = $[TrpRS]_{total}$. Then:

$$K_D = Kd_{\text{-EDTA}} = \{([D]_{tot} - x)^* ([Mg]_{tot} - x - y)\} / x$$

$$K_E^{\ddagger}=Kd_{\_\ TrpRS\bullet Mg\bullet ATP}=\{([E]_{tot}-y)^{*}([Mg]_{tot}-x-y)\}/y$$

Solving for y in terms of x:

$$y=K_D\bullet[E_{tot}]\bullet x/\left(K_E^{\ddagger}\bullet[D_{tot}]+K_D\bullet x-K_E^{\ddagger}\bullet x\right) \quad \text{(II)}$$

x can be obtained by solving iteratively the resulting quadratic expression in x and y from an initial estimate for y.

$$K_D\bullet x=D_{tot}\bullet M_{tot}-D_{tot}\bullet x-D_{tot}\bullet y-M_{tot}\bullet x+x\bullet y+x^2$$

$$0=x^2-(K_D+D_{tot}+M_{tot}-y)\bullet x+D_{tot}(M_{tot}-y)$$

$$x=\left\{(K_D+D_{tot}+M_{tot}-y)\pm sqrt\left\{(K_D+D_{tot}+M_{tot}-y)^2-4\bullet D_{tot}\bullet M_{tot}+4\bullet D_{tot}\bullet y\right\}\right\}/2$$

At convergence, solving (II) affords y, which can be substituted into (I) to obtain the calculated activity. The fitting process is summarized in Figure 4.

We programmed macros in the Excel program[32] to iterate solutions for the two quadratic equilibrium equations for each [EDTA] in Figure 1 and to evaluate equation (I) and the sum of squared errors (SSE) with respect to the observed activity values. A simplex algorithm was applied manually to search for a least squares solution, whose fitted parameters are given in Table 1.

Statistical Evaluation: numerical evaluation of the Hessian matrix for the SSE surface

The algorithm described above is both nonlinear and nested by the dependence of metal activated activity on the affinity parameter, $K_E^{\ddagger}$, requiring solution of equation (II) each time its value is adjusted. It is therefore beyond commercially available statistics software usually used to evaluate significance. We therefore used the programmed Excel worksheet for this purpose. The R^2 value is 0.990 implying that the model parameters explain all but 1% of the variability in the experimental observations. To assess the robustness of the solution, we determined the Hessian matrix numerically, using the Excel program to evaluate the SSE on a grid of 48 points surrounding the least squares solution. The resulting SSE values were fitted to an exact, bivariate quadratic polynomial in $K_E^{\ddagger}$ and R ($R^2 = 0.998$) whose coefficients were all determined with t-test probabilities < 0.0001 (JMP;33). Cross sections of this SSE surface are shown in the inset to Figure 1b. Its global minimum coincides with the least squares solution, and its curvature in the neighborhood of the minimum provides relative standard deviations of 35% (KD_{TS}) and 70% (R) for the parameter estimates (Table 1).

Acknowledgments

This work was supported by NIHGMS 48519 and 78227. We thank K. Levine and A. Essader at Research Triangle Institute, RTP, NC for ICP-OESL analyses. We thank M. Forconi for suggesting models for uncatalyzed amino acid

activation rates, M. Caplow for critical insights, and R. Wolfenden for discussion and encouragement, and for his example.

References

(1). Tetas M, Lowenstein JM. Biochem 1963;2:350–357. [PubMed: 13980762]
(2). Fothergill M, Goodman M, Petruska J, Warshel A. J. Am. Chem. Soc 1995;117:11619–11627.
(3). Åqvist J, Warshel A. J. Am. Chem. Soc 1990;112:2860–2868.
(4). Beese LS, Steitz TA. EMBO J 1991;10:25–33. [PubMed: 1989886]
(5). Saderholm MJ, Hightower KE, Fierke CA. Biochem 2000;39:12398–12405. [PubMed: 11015220]
(6). Leatherbarrow RJ, Fersht AR, Winter G. Proc. Nat. Acad. Sci., USA 1985;82:7840–7844. [PubMed: 3865201]
(7). Kirby AJ, Varvaoglis AG. J. Am. Chem. Soc 1967;89:415–423.
(8). Kirby AJ, Younas M. Journal of the Chemical Society 1970;B 418:1165–1172.
(9). First EA, Fersht AR. Biochem 1995;34:5030–5043. [PubMed: 7711024]
(10). Hu, H.; Yang, W. Quantum mechanical/molecular mechanics simulations of tryptophan activation by Tryptophanyl-tRNA synthetase. Duke Universityunpublished work in progress
(11). Fersht AR. Biochem 1987;26:8031–8037. [PubMed: 3442641]
(12). Fersht AR, Knill Jones JW, Bedouelle H, Winter G. Biochem 1988;27:1581–1587. [PubMed: 3284584]
(13). Kapustina M, Carter CW Jr. J. Mol. Biol 2006;362:1159–1180. [PubMed: 16949606]
(14). Retailleau P, Huang X, Yin Y, Hu M, Weinreb V, Vachette P, Vonrhein C, Bricogne G, Roversi P, Ilyin V, Carter CW Jr. J. Mol. Biol 2003;325:39–63. [PubMed: 12473451]
(15). Retailleau P, Weinreb V, Hu M, Carter CW Jr. J. Mol. Biol 2007;369:108–128. [PubMed: 17428498]
(16). Carter, CW, Jr.. The Aminoacyl-tRNA Synthetases. Ibba, M.; Francklyn, C.; Cusack, S., editors. Landes Biosciences/ Eurekah.com; Georgetown, TX: 2005. p. 99-110.
(17). Levitt M, Warshel A. J. Mol. Biol 1976;103:227–249. [PubMed: 985660]
(18). Cohn M. Annals of the New York Academy of Sciences 1990;603:151–164. [PubMed: 2291517]
(19). Adolfson R, Moudrianakis E. J. Biol. Chem 1978;253:4378–4379. [PubMed: 659423]
(20). Invitrogen. The Handbook - A Guide to Fluorescent Probes and Labeling Technologies. Invitrogen Corporation; 2005.
(21). Holmquist B. Meth. Enz 1981;158:6–12.
(22). Admiraal SJ, Herschlag D. Chem Biol 1995;2:729–739. [PubMed: 9383480]
(23). Doublie S, Bricogne G, Gilmore C, Carter CW Jr. Structure 1995;3:17–31. [PubMed: 7743129]
(24). Retailleau P, Yin Y, Hu M, Roach J, Bricogne G, Vonrhein C, Roversi P, Blanc E, Sweet RM, Carter CW Jr. Acta Cryst 2001;57:1595–1608.
(25). Carter, P. a.; W., JA. Nature 1988:564–568. [PubMed: 3282170]
(26). Chan KW, Koeppe RE. Biochim. Biophys. Acta 1994;1205:223–229. [PubMed: 8155701]
(27). Chan KW, Koeppe RE. FEBS Lett 1995;363:33–36. [PubMed: 7729548]
(28). Kapustina M, Weinreb V, Li L, Kuhlman B, Carter CW Jr. Structure 2007;15:1272–1284. [PubMed: 17937916]
(29). Pham Y, Li L, Kim A, Weinreb V, Butterfosss G, Kuhlman B, Carter CW Jr. Molecular Cell 2006;25:851–862. [PubMed: 17386262]
(30). Sillen, LG.; Martell, AE. Stability Constants of Metal Ion Complexes. The Chemical Society; London, UK: 1964.
(31). Patton C, Thompson S, Epel D. Cell Calcium 2004;35:427–431. [PubMed: 15003852]
(32). Microsoft; Seattle, WA: 2002.
(33). SAS. V.6 ed.. SAS; Cary, NC: 2004.
(34). Synergy. 4.01 ed.. Synergy Software; Reading, PA: 2005.

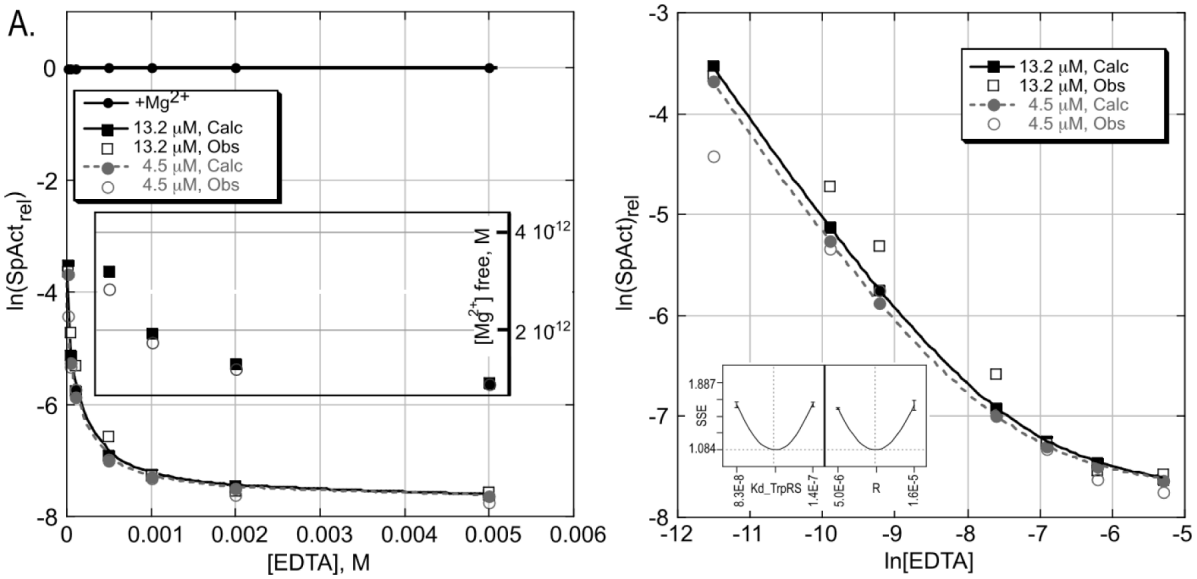

Figure 1.

[EDTA]-dependence of relative TrpRS catalytic activity. A. EDTA has no effect on activity if an excess of Mg^{2+} is present. Activity in Mg^{2+}-depleted assays (relative specific activity, derived by dividing Act_{obs} in equation (I) by WT activity) falls to a plateau with increasing [EDTA]. This plateau activity remains ~10^{10} times that of the uncatalyzed reaction. The insert shows the $[Mg^{2+}]_{free}$ calculated by the regression model. B. A ln-ln plot emphasizes differences between the model and the experimental data, showing the intrinsic variation in the data and quality of the fit. Although the data for the higher [TrpRS] appears to deviate systematically from the fitted line, the errors are random, so far as we can tell. Plotted curves pass through the calculated model values (solid characters); the data are open characters. Insert shows the curvature of the sum of squared errors vs values of the two fitted parameters. The breadths of these response surface sections are related to the estimated uncertainties. Graphs were prepared using Kaleidagraph[34].

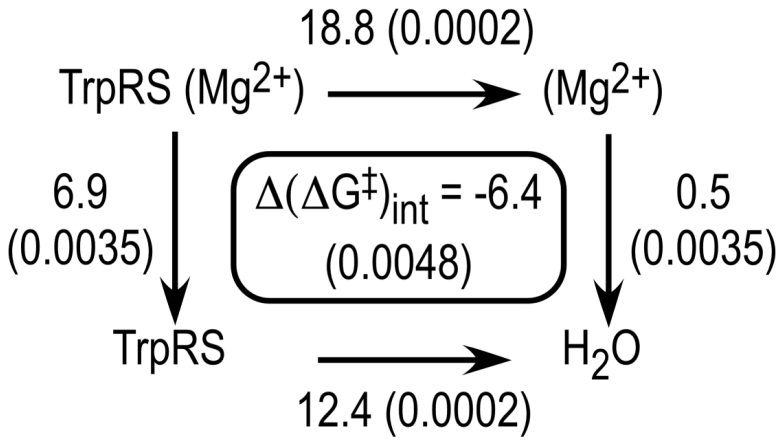

Figure 2.
Double variant thermodynamic cycle describing the free energies of transition state stabilization due to the TrpRS polypeptide, to the Mg^{2+}, and to their interaction ($\Delta(\Delta G_{int})$). Free energies in Kcal/Mole and (t-test probabilities) were estimated using bivariate multiple regression (JMP;33). $R^2 = 0.999$ for the model, with P(F) = 0.0006.

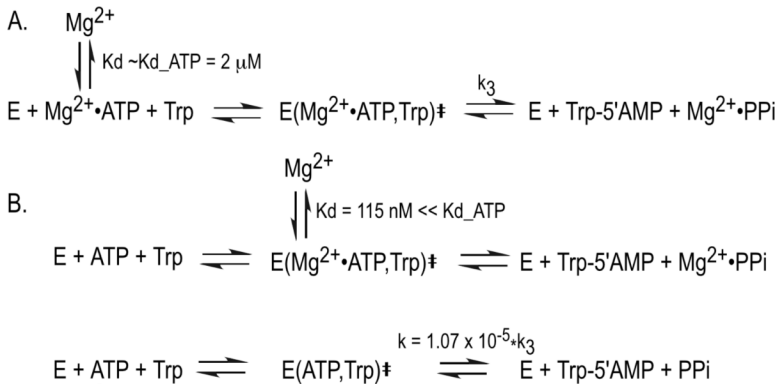

Figure 3.

Kinetic scheme for TrpRS PPi exchange activity under conditions of depleted [Mg^{2+}]. A. Tryptophan activation in the presence of saturating [Mg^{2+}]. The Km for Mg^{2+} is comparable to that for the dissociation of Mg^{2+} from ATP and may therefore be conditioned by that equilibrium. B. Parallel activities of Mg^{2+}•ATP and metal-free ATP. In this case, Mg^{2+} is recruited in the transition state complex which binds metal an order of magnitude more avidly, consistent with the [EDTA] dependence of the reaction in Mg^{2+}-depleted assays. The metal-free reaction is slower by ~ five orders of magnitude, and so contributes little to the reaction in the absence of EDTA and begins to contribute significantly when the fraction of Mg^{2+}-activated enzyme falls below about 10^{-4}. Equilibria and relative rate parameters (Table 1) are derived by non-linear regression, as described.

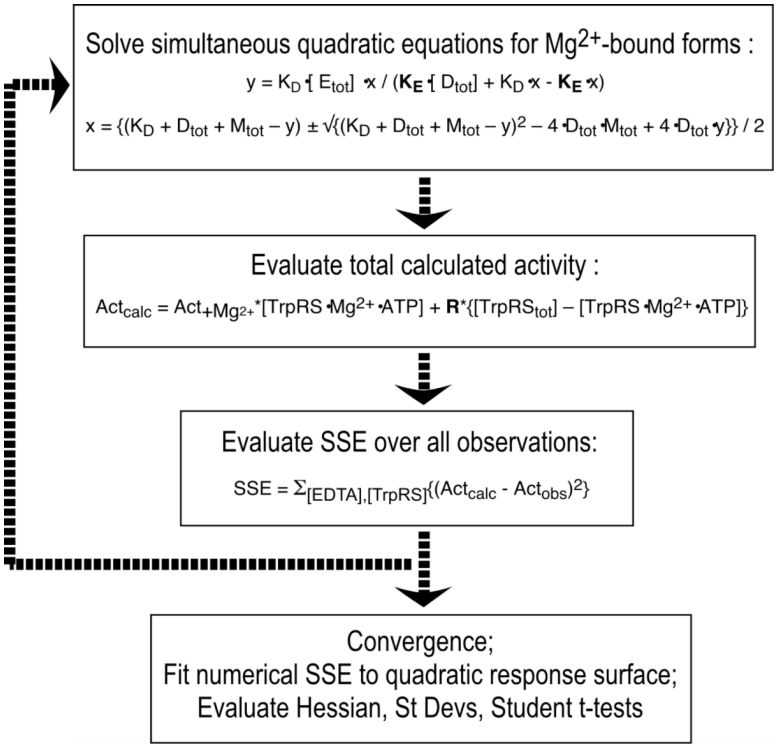

Figure 4.

Iterative fitting of observed catalytic activity with increasing [EDTA]. Three separate stages are required because the two unknown parameters (bold face) are embedded in different relationships. Concentrations of the bound forms are involved in simultaneous nonlinear relationships that must be evaluated before the (linear) dependence of the observed activity on Mg^{2+}-bound TrpRS•ATP•Trp can be assessed.

Table 1

Least Squares Parameters for Recursive, Nonlinear Estimation of Activity

Parameter	Fitted value	Standard Deviation	% error
$K_E^{\ddagger}$ (TrpRS•Mg•ATP)	1.15E-7 (M)	± 4.0E-8 (M)	35
R	0.0000107	± 7.5E-6	70

Table 2

Analytical Mg^{2+} Determination (ICP-OES) of Assay samples

Sample	$[Mg^{2+}]$, ug/mL[a]	$[Mg^{2+}]$, M
ddH_2O	0.0155±0.0035	6.52E-7
Buffer	0.011±0.0035	4.63E-7
TrpRS	0.032±0.002	2.30E-8; 6.67E-7
PPi	0.022±0.004	7.58E-08
EDTA	0.091±0.005	Variable; <1.83E-06

[a]Determined by K. Levine and A. Essader, Research Triangle Institute, RTP, NC

Table 3

Mg^{2+} Dissociation Constants Relevant to the Observed TrpRS Activity in Figure 1.

Compound	Kd, M	Source; comments
ATP	6.0×10^{-5}	30
	7.0×10^{-6}	19
Pyrophosphate	2.0×10^{-6}	30
EDTA	2.0×10^{-9}	30
TrpRS•ATP	2.0×10^{-6}	14; Km, determined by Michaelis-Menten kinetics